JOURNAL OF MATERIALS SCIENCE 32 (1997) 5645–5651

Surface study of a titanium-based ceramic electrode material by X-ray photoelectron spectroscopy

J. POUILLEAU, D. DEVILLIERS*, H. GROULT
Université Pierre et Marie Curie Laboratoire d'Electrochimie CNRS URA 430 4, Place Jussieu, 75252 Paris Cedex 05, France

P. MARCUS
E. N. S. C. P., Laboratoire de Physicochimie des surfaces, CNRS URA 425 11, Rue Pierre et Marie Curie, 75231 Paris Cedex 05, France

The electrochemical behaviours of the Magnéli phase titanium oxides with the general formula Ti_xO_{2x-1} have been investigated. Surface analysis of these ceramic materials was performed using X-ray photoelectron spectroscopy in order to determine the surface composition. It was shown that the surface layers contain mainly Ti^{IV}. When these materials are used as an anode for oxygen evolution, in sulfuric acid, the XPS spectrum shows considerable modification in the O1s region, due to an important contribution of hydroxyl groups and the adsorption of sulfate anions.

1. Introduction

The application of ceramic materials in electrochemical devices has been an area of study for more than 20 years. The Magnéli phase titanium oxides with the general formula Ti_xO_{2x-1} ($4 \leqslant x \leqslant 10$) are commercially available materials that find use as bulk electrode materials. Their properties have been extensively studied [1–3] and their applications, especially in environmental electrochemical technology, have been reported in review papers [4, 5].

The kinetics of several redox couples (ferro/ferricyanide [3] and Ce^{4+}/Ce^{3+} [2]) on bare titanium oxide electrodes are reported to be slow compared with platinum electrodes. It has been suggested [2] that this behaviour is related to the formation of less conducting titanium oxide layers (more oxidized) on the surface of the electrode. Indeed, it is well known that stoichiometric titanium dioxide is a poor conductor.

In this paper, X-ray photoelectron spectroscopy (XPS) is used to probe whether or not oxidation of the surface of the electrodes actually occurs when they are used as anodes. The results are compared with those obtained with a Ti/TiO_2 surface electrode.

2. Experimental details

In the following experiments the properties of ceramic samples of Ti_4O_7 and Ti_5O_9 are probed. These samples were prepared from two kinds of Ebonex™ plates, provided by Atraverda Ltd: "porous" Grade 1 (porosity 20%) and "non porous" Grade 2 (porosity 0.1–4%).

2.1. Scanning electron microscopy (SEM)

As was expected, the "porous" grade sample (see Fig. 1a) contained a significant number of holes with an average diameter of 2 μm. The "non-porous" sample was polished with silicon oxide paper (Buehler fibrmet 3 μm) before being examined by SEM. This sample contains only a few pores on the surface (see Fig. 1b) but a cross-sectional view (Fig. 1c) shows that these pores can be very deep.

2.2. Electrochemical experiments

The ceramic samples were tested by making them working electrodes. The porous grade material formed electrodes 1 and 2 whilst the non porous material was used for electrodes 3 and 4.

A saturated sulfate reference electrode (SSE) and a platinum counter electrode were used in all these experiments. All the measured potentials will be referred to the SSE hereafter (+0.66 V versus the normal hydrogen electrode NHE). Cyclic voltammograms were measured at a low sweep rate ($v = 0.3\ mV\ s^{-1}$) using 0.5 M sulfuric acid as the electrolyte.

2.3. X-ray photoelectron spectroscopy

The "non porous" ceramic samples were analysed by X-ray photoelectron spectroscopy (XPS), using a VG Scientific ESCALAB Mark II Spectrometer equipped with two ultrahigh-vacuum (UHV) chambers, one for sample preparation and one for sample analysis. A MgK_α X-ray source was used. The analyser was

* Author to whom correspondence should be addressed.

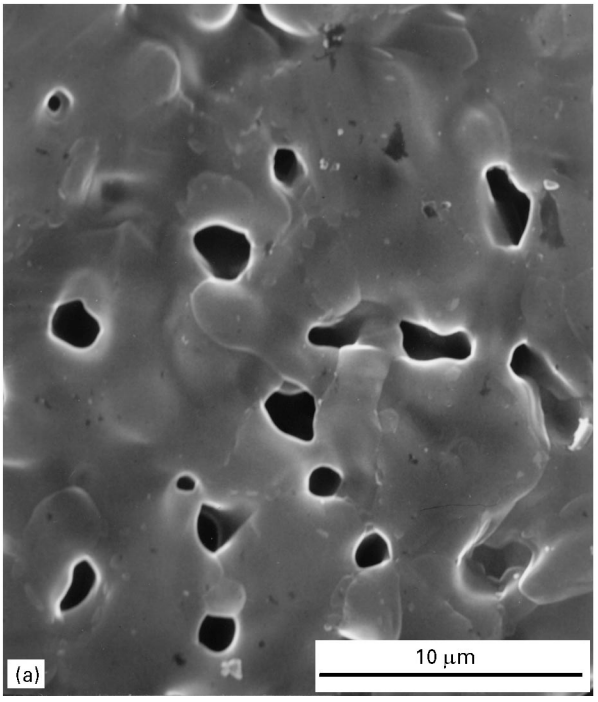

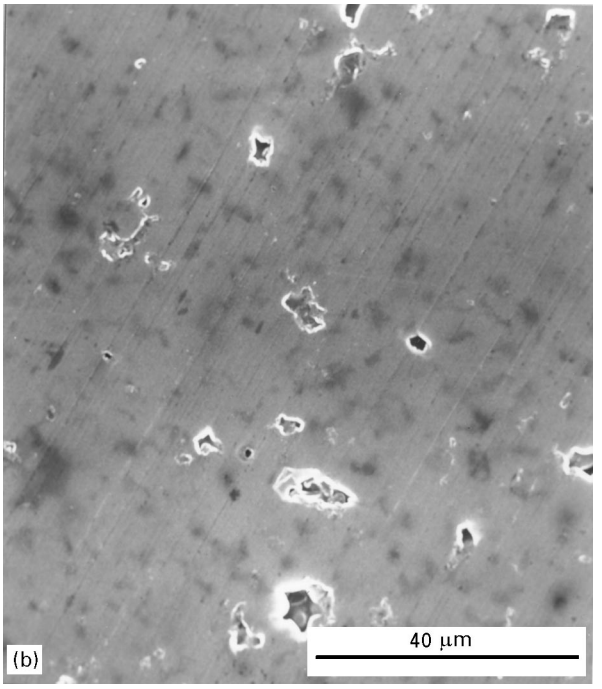

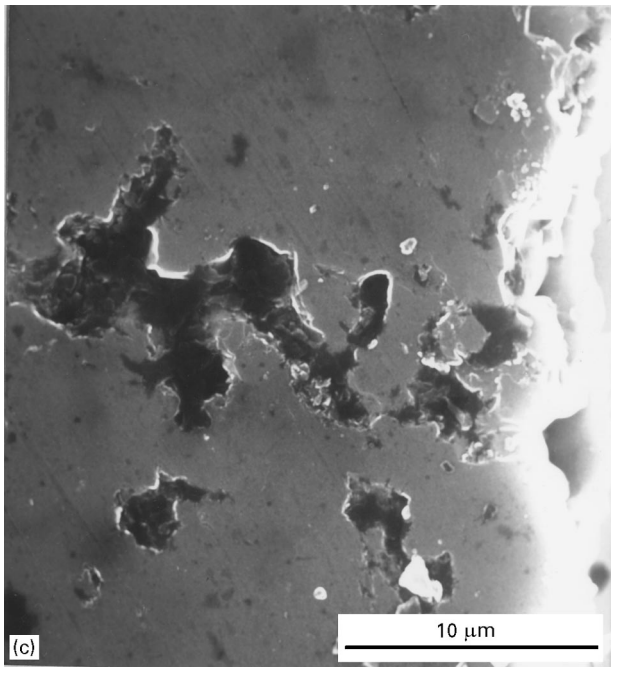

Figure 1 Micrographs of titanium-based ceramics, (a) "porous" grade; (b) "non porous" grade; polished sample and (c) "non porous", cross-section.

operated at 20 eV pass energy for high resolution spectra and at 50 eV for survey spectra. The analysed area was 10 mm^2. The angle-resolved measurements were carried out at two different electron take-off angles, θ of 90 or 40°. The reference energies used for calibration were the $Au4f_{7/2}$ signal at a binding energy, E_b 83.9 eV and the $Cu2p_{1/2}$ signal at E_b = 932.7 eV.

A ceramic sample was polished with a Buehler "fibrmet" paper (SiO_2 granulometry 3 μm). It was rinsed with distilled water, cleaned in absolute ethanol with an ultrasonic cleaner and rinsed again with distilled water. This sample is designated as sample 1. Two polished ceramic samples were used as electrodes in a cell containing 0.5 M sulfuric acid at 25 °C. A 5 V bias was applied for 3 h between these two electrodes. Oxygen evolution occurred on the anode and hydrogen on the cathode. After this operation, the electrodes were carefully rinsed and studied by XPS. The anode is designated as sample 2 and the cathode as sample 3.

The results obtained with these samples were compared with those obtained with other kinds of titanium oxides. A polycrystalline titanium foil (Goodfellow; purity 99.6%) was polished with silicon carbide abrasive paper and Buehler alumina suspensions (granularity 1 and 0.3 μm). After polishing, the sample was cleaned as described above. During the polishing treatment, a thin layer of titanium oxide is formed on the surface of the metal. The freshly polished titanium foil is designated as sample 4. A thick TiO_2 layer was prepared by electrochemical oxidation of a polished titanium electrode, using a constant current density, j, of 5 mA cm^{-2}, in 0.5 M sulfuric acid, at 25 °C, under an argon atmosphere. The oxidation step was stopped when the potential of the working electrode reached 20 V versus the Pt counter electrode. Using these experimental conditions, it has been previously shown [6] that the amorphous oxide layer is about 60 nm thick. The current efficiency for the anodic formation of TiO_2 was only about 85%, due to an oxygen evolution side-reaction, as has been described in the literature [7–9]. The Ti/electrogenerated TiO_2 sample is designated as sample 5.

3. Results

3.1. Electrochemical experiments

The plots obtained with the two porous ceramic working electrodes (electrodes 1 and 2) are presented in Fig. 2a. Electrode 1 was submitted to one anodic scan

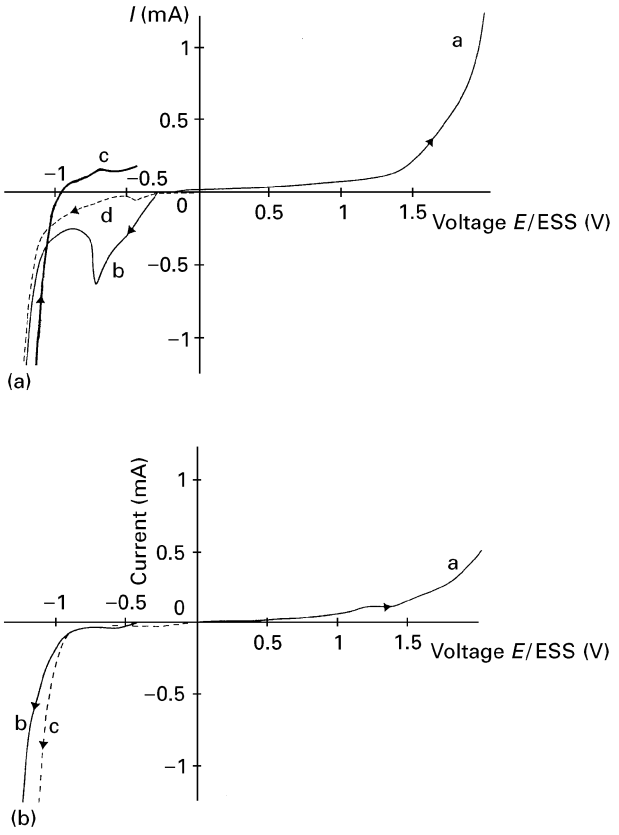

Figure 2 *I–E* curves for ceramic electrodes in 0.5 mol l^{-1} H_2SO_4; (a) "porous" grade samples; electrode (3) area $S = 0.3\ cm^2$; electrode 1 (full lines): anodic scan (a); cathodic scan (b); reverse scan (c); electrode 2 (dotted line): cathodic scan only (d). (b) "non porous" grade samples; $S = 0.6\ cm^2$; electrode 3: anodic scan (a); cathodic scan (b); electrode 4: cathodic scan only (c).

(a), from the rest potential (-0.2 V) to 2 V, and then to a cathodic scan (b) from the rest potential to -1.5 V, and finally to the reverse scan -1.5 to -0.4 V (c). Oxygen evolution occurs at potentials, $E > 1.5$ V and hydrogen evolution occurs at $E < -1.1$ V. A broad cathodic peak is observed during the reduction step, at about -0.7 V which is attributed to the multi-step reduction of the oxygen evolved during the first anodic scan and still present in the pores. This peak is not present if the electrode is not subjected to oxygen evolution: see the curve corresponding to electrode 2. It can also be seen that hydrogen evolution occurs at higher potentials on the reverse scan -1.5 to -0.2 V.

The same kind of curves were obtained with the non porous ceramic electrodes, except for the occurrence of the cathodic peak (See Fig. 2b). It was also observed that hydrogen evolution occurs more easily on a fresh electrode (electrode 4, curve c) rather than on an electrode on which oxygen evolution occurred at 2 V for 30 min (electrode 3, curve b). For example, for a current density, j, of $-1\ mA\ cm^{-2}$ the potentials were respectively -1.05 and -1.15 V. All these results are in agreement with those previously reported [2] and seem to indicate that the surfaces of the electrodes are somewhat passivated after the occurrence of a strong oxygen evolution. This point will be discussed in detail later.

3.2. Surface analysis

3.2.1. Survey spectra

The survey spectra obtained with samples 1, 2 and 3 are very similar. The spectrum corresponding to sample 2 is presented as Fig. 3. The Ti2p photoelectron peaks at a binding energy, E_b, of 458 eV and those of O1s at $E_b = 531$ eV are clearly observed. The high resolution spectra of the Ti2p and O1s regions are shown in Figs 4 (a and b) and 5 (a–d). Carbon from a thin contamination layer is also present on all the spectra.

The Auger peaks O(A), C(A) and Ti(A) are also present in the spectra at higher energies, but they will not be considered in the following discussion.

Sulfur peaks are observed in the spectra of samples 2 and 3. They are attributed to the contamination

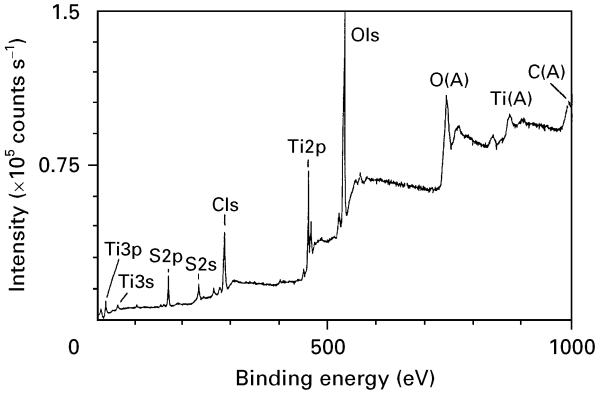

Figure 3 XPS survey spectrum for a titanium-based ceramic used as an anode in 0.5 mol l^{-1} H_2SO_4 (sample 2).

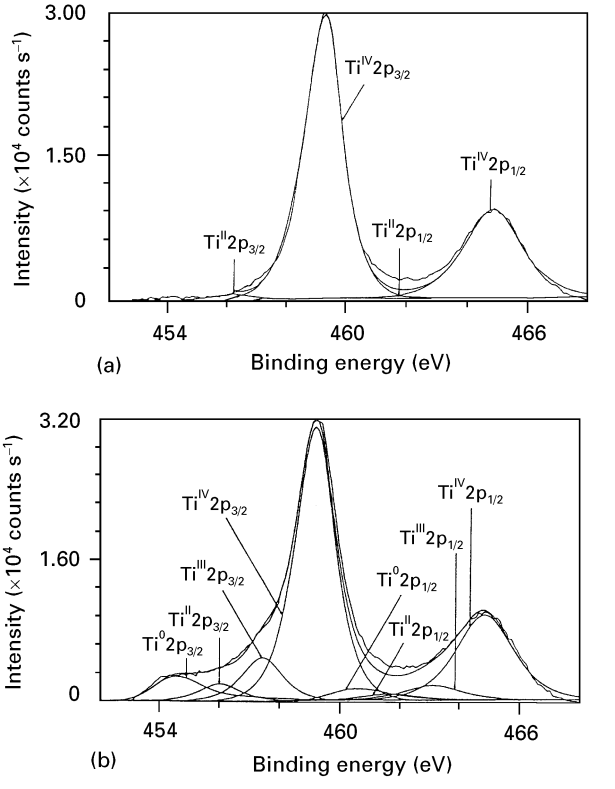

Figure 4 XPS spectra of the Ti2p region; (a) titanium-based ceramic (sample 1) and (b) polished titanium foil (sample 4).

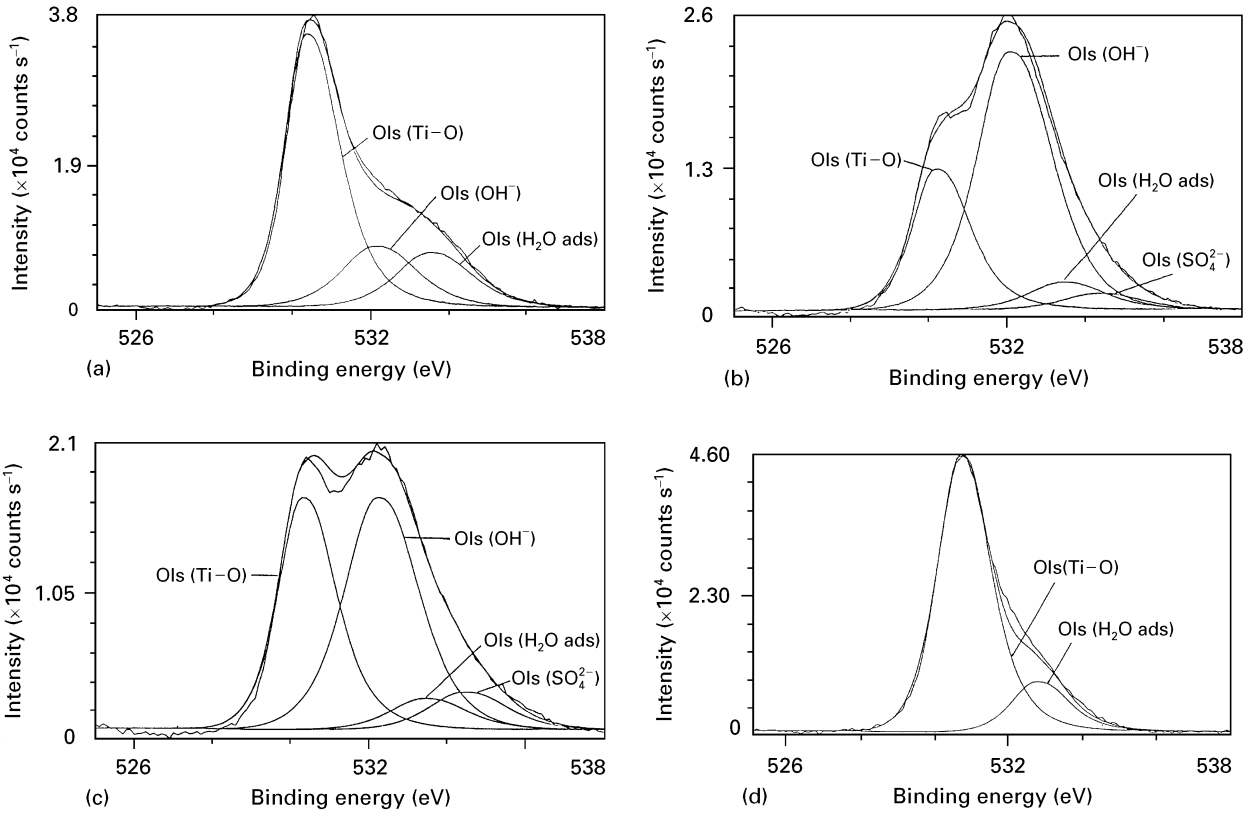

Figure 5 XPS spectra of the O1s region; (a) sample 1 (ceramic); (b) sample 2 (ceramic used as anode); (c) sample 3 (ceramic used as cathode) and (d) sample 4 (polished titanium foil).

of the surface by sulfate and to the diffusion of H_2SO_4 into the bulk of the ceramic during the experiment in the electrochemical cell. Indeed, the diffusion of the acidic electrolyte into the electrode material occurs even in the "porous grade" samples. In fact the corrosion of the copper contact between the current lead and the electrode was observed after long experiments.

3.2.2. High resolution spectra

3.2.2.1. The Ti2p region. The Ti2p region can be decomposed into several contributions corresponding to the different oxidation states of titanium. Each contribution consists of a doublet between the $2p_{3/2}$ and $2p_{1/2}$ peaks. For each doublet, the ratio of the area of the two peaks $A(Ti2p_{1/2})/A(Ti2p_{3/2})$ is equal to 0.5 and the binding energy difference, $\Delta E_b = E_b(Ti2p_{1/2}) - E_b(Ti2p_{3/2})$ is always 5.7 eV, as previously reported in the literature [10].

The spectrum corresponding to sample 1 is shown in Fig. 4a. It is characterized by a main doublet composed of two symmetric peaks situated at $E_b(Ti2p_{3/2}) = 459.2$ eV and $E_b(Ti2p_{1/2}) = 464.9$ eV, in agreement with the literature [10, 11]; this main doublet is assigned to Ti^{IV} (titanium in the IV oxidation state). It was found that the spectra of samples 1, 2, 3 and 5 all contain this doublet as their major feature. In addition, it is also necessary to take into account a minor contribution from Ti^{II}. The individual fitting parameters (binding energies, E_b and the full width at half-maximum peak height, FWHM) are listed in Table I.

The spectrum of sample 4, shown in Fig. 4b, is however more complicated. Its complete decomposition is presented in Fig. 4b. Several minor contributions were found, they include: (i) Ti^{III} from Ti_2O_3 species. The symmetric peaks of the corresponding doublet are situated at $E_b(Ti2p_{3/2}) = 457.4$ eV and $E_b(Ti2p_{1/2}) = 463.1$ eV, as reported in the literature [11]. (ii) Ti^{II} from TiO species. The two symmetric peaks of the doublet have the following binding energies: $E_b(Ti2p_{3/2}) = 456$ eV and $E_b(Ti2p_{1/2}) = 461.7$ eV [11]. (iii) Ti^0 from metallic titanium. This last doublet is composed of two asymmetric peaks at $E_b(Ti2p_{3/2}) = 454.4$ eV and $E_b(Ti2p_{1/2}) = 460.4$ eV, as is usual in the case of a metal in the 0 oxidation state [10, 11]. The Ti^0 peaks are observed in the spectrum because the oxide film is thin. Its thickness was evaluated to be about 6 nm from XPS measurements [6].

The binding energy corresponding to each peak, and the binding energy difference ΔE_b between the two peaks of each doublet are in agreement with values reported in the literature [10–13].

The results of the decomposition of the spectrum of sample 5 (electrogenerated titanium oxide) are also presented in Table I. The main peaks (Ti^{IV} doublet) are situated at $E_b(Ti2p_{3/2}) = 458.8$ eV and $E_b(Ti2p_{1/2}) = 464.5$ eV in agreement with the literature [10, 12]. These values are slightly lower than those obtained with the ceramic samples (1, 2 and 3) but they are almost identical if the error range is considered.

TABLE I Peak fitting parameters of the high resolution spectrum of the Ti2p region for samples 1–5 for a take-off angle $\theta = 90°$ (accuracy: $E_b \pm 0.2$ eV). r_i (%) represents the ratio $A_i/\Sigma A_i$ (relative contribution of each peak in a same sample); FWHM is the full-width at half-maximum

		$Ti^{IV}2p_{3/2}$	$Ti^{IV}2p_{1/2}$	$Ti^{III}2p_{3/2}$	$Ti^{III}2p_{1/2}$	$Ti^{II}2p_{3/2}$	$Ti^{II}2p_{1/2}$	$Ti^{0}2p_{3/2}$	$Ti^{0}2p_{1/2}$
FWHM (eV)		1.6	2.3	1.6	2.3	1.6	2.3	2.0	2.2
	E_b (eV)	459.2	464.9	–	–	456.0	461.7	–	–
Sample 1	A_i (cs^{-1} eV)	51 460	24 755	–	–	2170	1065	–	–
	r_i (%)	96		–		4		–	
	E_b (eV)	459.0	464.7	–	–	–	–	–	–
Sample 2	A_i (cs^{-1} eV)	23 725	11 915	–	–	–	–	–	–
	r_i (%)	100		–		–		–	
	E_b (eV)	459.0	464.7	–	–	456.0	461.7	–	–
Sample 3	A_i (cs^{-1} eV)	25 430	12 095	–	–	645	345	–	–
	r_i (%)	97		–		3		–	
	E_b (eV)	459.1	464.8	457.4	463.1	456.0	461.7	454.4	460.4
Sample 4	A_i (cs^{-1} eV)	55 340	24 560	8590	4235	3350	1715	5890	3205
	r_i (%)	75		5		12		8	
	E_b (eV)	458.8	464.5	457.4	463.1	456.0	461.7	–	–
Sample 5	A_i (cs^{-1} eV)	51 940	24 895	645	315	685	375	–	–
	r_i (%)	98		1		1			

Minor contributions from Ti^{III} and Ti^{II} have been considered, but Ti^0 is not present since the titanium substrate cannot be detected because the oxide film is too thick. Its thickness was evaluated to be about 60 nm by Rutherford backscattering experiments, and the attenuation length of the Ti2p photoelectrons in titanium oxide was estimated to be 2.1 nm [6].

The peak parameters presented above were useful in the fitting of the high resolution spectra obtained with samples 1, 2 and 3. For these three ceramic samples, there is no contribution from Ti^0 and the small contribution from Ti^{III} was omitted.

For sample 1, the spectrum is almost identical to that of TiO_2 (sample 5) within the experimental accuracy ± 0.2 eV (see Table I and Fig. 4a). The bulk composition of the ceramic is Ti_xO_{2x-1} ($4 \leqslant x \leqslant 10$); however, the spectrum indicates that the surface of the ceramic sample behaves as TiO_2 (96%) with a small percentage of lower oxidation states of titanium (4%). The accuracy is not sufficient to distinguish between Ti^{II} and Ti^{III}. Only Ti^{II} has been considered in this case.

For samples 2 and 3, the appearance of each spectrum is identical to that of sample 1. As it can be seen from Table I, the relative ratio of each peak contribution, r_i, is almost identical.

3.2.2.2. The O1s region. It has been shown previously that the spectra of the ceramic samples in the Ti2p region look like the spectrum of electrogenerated TiO_2. So, we have compared the high resolution spectra of the O1s region of samples 1, 2, 3 and 4 and they are presented in Fig. 5 (a–d).

The O1s spectra have been decomposed into several contributions. The results are presented in Table II. For samples 1, 4 and 5, the main contribution is attributed to Ti–O bonds and minor contributions of OH groups belonging to hydroxyl groups or adsorbed H_2O must also be considered. On the contrary, for samples 2 and 3, the spectra of the O1s region are quite different and a major contribution from OH groups can be observed for sample 2. Although Ti is always present in the IV oxidation state, the species present at the surface of the samples used as electrodes in sulfuric acid are modified.

For sample 1 (see Fig. 5a), three oxygen contributions were taken into account: (i) from Ti–O bonds, (ii) from hydroxyl groups, and (iii) from adsorbed H_2O. The last two contributions correspond to surface groups, because, as can be seen in Table II, their ratios r_i increase with a decrease in the take-off angle θ.

For samples 2 and 3, a new contribution had to be added to produce a better fit of the spectra at $E_b = 534.3 \pm 0.1$ eV. This is attributed to sulfur–oxygen bonds from SO_4^{2-} species adsorbed onto the surface of the electrodes or inserted deeper into the ceramic bulk through the pores. The relative contributions of Ti–O bonds have decreased and OH groups have increased, especially for the sample used as a cathode, in the electrochemical experiments.

3.2.2.3. Composition of the titanium compounds. Titanium oxides. The high resolution spectra of the O1s region for samples 4 and 5 exhibit a contribution attributed to Ti–O bonds and a smaller contribution due to adsorbed H_2O. It can be concluded that these samples contain only titanium oxides and no hydroxides. The high resolution spectra of the Ti2p region for the samples give information on the oxidation degree of the surface compounds: thick layers of electrogenerated titanium oxides (sample 5) are mainly composed of insulating TiO_2 (98%). During the polishing treatment, a titanium oxide is formed on the titanium foil, mainly composed of TiO_2, but minor contributions of Ti^{II} and Ti^{III} titanium suboxides must also be taken into account.

TABLE II Peak fitting parameters for the O1s region (accuracy: $E_b \pm 0.5$ eV) for ceramic samples (1, 2 and 3) and oxidized titanium substrates (samples 4 and 5). r_i (%) represents the ratio $A_i/\Sigma A_i$ (relative contribution of each peak in a sample); FWHM is the full-width at half-maximum

Ceramic samples		O1s (Ti–O)	O1s (OH^-)	O1s (H_2O ads)	O1s (SO_4^{2-})
FWHM (eV)		1.7	2.3	2.3	2.3
	E_b (eV)	530.4	532.1	533.5	–
Sample 1 ($\theta = 90°$)	A_i (cs^{-1} eV)	64 650	19 840	17 800	–
	r_i (%)	63	19	18	–
	E_b (eV)	530.5	532.1	533.6	–
Sample 1 ($\theta = 40°$)	A_i (cs^{-1} eV)	41 105	17 110	17 110	–
	r_i (%)	55	23	23	–
	E_b (eV)	530.2	532.1	533.4	534.3
Sample 2 ($\theta = 90°$)	A_i (cs^{-1} eV)	24 050	56 670	6145	3620
	r_i (%)	27	63	7	4
	E_b (eV)	530.3	532.2	533.4	534.4
Sample 3 ($\theta = 90°$)	A_i (cs^{-1} eV)	32 425	42 376	5746	7010
	r_i (%)	37	48	7	8
Titanium oxides		O1s (Ti–O)	O1s (OH^-)	O1s (H_2O ads)	O1s (SO_4^{2-})
FWHM (eV)		1.5	–	1.6	–
	E_b (eV)	530.6	–	532.7	–
Sample 4 ($\theta = 90°$)	A_i (cs^{-1} eV)	87 640	–	16 960	–
	r_i (%)	84	–	16	–
	E_b (eV)	530.2	–	532.4	–
Sample 5 ($\theta = 90°$)	A_i (cs^{-1} eV)	63 310	–	19 800	–
	r_i (%)	76	–	24	–

Ceramic titanium suboxides. The analysis of the Ti2p region proves that the surface of the three ceramic samples (1, 2 and 3) contain mainly Ti^{IV} (96%), although the bulk composition of Ti_xO_{2x-1} is not expected to contain such large amounts of Ti^{IV}: (i) for $x = 4$, the theoretical composition of the bulk of the Ti_4O_7 ceramic is $Ti_3^{IV}Ti^{II}O_7$; i.e., 75% Ti^{IV} whilst (ii) for $x = 10$, the composition is $Ti_9^{IV}Ti^{II}O_{19}$; i.e., 90% Ti^{IV}.

For the samples under study ($4 \leq x \leq 10$), the experimental results (Ti2p region) show that the surface of the electrode is more oxidized than the bulk. We have observed that the spectra of the Ti2p region are exactly the same for polished or non polished ceramic samples. It can be deduced that the oxidation of the surface of the samples is not related to their polishing treatment.

The analysis of the O1s region shows the occurrence of the OH groups, especially for the ceramic samples used as an anode (sample 2) or cathode (sample 3) in the electrochemical experiments. It can be concluded that titanium hydroxides are now present at the ceramic/electrolyte interface rather than TiO_2 as in the case of an oxidized titanium electrode (samples 4 and 5). This major difference between the two kinds of samples may explain why they have a different electrochemical behaviour: Ti/TiO_2 anodes are strongly passivated [6] and ceramic titanium suboxide anodes are not.

4. Conclusions

Polished titanium is covered by a layer of titanium dioxide containing other titanium suboxides as minor components. Electrogenerated titanium oxide is mainly composed of TiO_2 ($\approx$98%). In the same way, the surface of all the ceramic samples under study contain mainly Ti^{IV}, although the bulk Ti_xO_{2x-1} ($4 \leqslant x \leqslant 10$) does not contain such large amounts of Ti^{IV}.

As the percentage of such contribution of the peaks in the Ti2p region does not vary from sample 1 (crude ceramic) to samples 2 (ceramic used as anode) and 3 (ceramic used as a cathode), it can be concluded that, in ceramic electrodes used as anodes or cathodes, the oxidation state of the Ti at the surface of the electrodes does not change notably.

On the contrary, the O1s region is strongly modified, indicating that the adsorption of oxygenated species on the electrode material is important and that hydroxyl groups from titanium hydroxide are now present, rather than titanium dioxide.

The XPS experiments on ceramic electrodes that had been used as anodes do not show any modification of the oxidation state of the titanium. Ti^{IV} already exists as a major component of the surface of the ceramic electrodes before the oxygen evolution. The slight passivation of ceramic titanium suboxide anodes is attributed to the presence of titanium hydroxide. It should be noted that OH^- groups are not present on Ti/TiO_2 electrodes, that are strongly passivated and cannot be used as anodes (electrogenerated TiO_2 is reported [13] to behave as a n-type semiconductor).

Acknowledgements

The authors thank Dr. R. Clarke (Atraverda Ltd) who provided the Ebonex™ samples. The experimental help of H. Cavalié (Laboratoire d'Electrochimie, U.P.M.C.) and C. Hinnen (Laboratoire de Physicochimie des surfaces, E.N.S.C.P.) is appreciated.

References

1. R. R. MILLER-FOLK, R. E. NOFTLE and D. PLETCHER, *J. Electroanal. Chem.* **274** (1989) 257.
2. J. E. GRAVES, D. PLETCHER, R. L. CLARKE and F. C. WALSH, *J. Appl. Electrochem.* **21** (1991) 848.
3. M. ZWEYNERT, H. DÖRING, J. GARCHE, R. A. HUGGINS and W. WITSCHEL, I. S. E. 4th Meeting, Berlin, abstracts (1993) 650.
4. R. L. CLARKE and S. K. HARNSBERGER, *Amer. Lab.* **20** (1988) 6.
5. R. CLARKE and R. PARDOE in "Electrochemistry for a cleaner environment", edited by D. Genders and N. Weinberg (Electrosynthesis, East Amherst NY, 1992) p. 349.
6. J. POUILLEAU, PhD thesis, University Pierre and Marie Curie, Paris, 1996.
7. J. L. DELPLANCKE and R. WINAND, *Electrochim. Acta* **33** (1988) 1539.
8. *Idem*, *ibid*. **33** (1988) 1551.
9. Y. SERRUYS, T. SAKOUT and D. GORSE, *Surf. Sci.* **282** (1993) 279.
10. C. D. WAGNER, W. M. RIGGS, L. E. DAVIS, J. F. MOULDERS and G. E. MULLENBERG, in "Handbook of X-ray photoelectron spectroscopy", edited by G. E. Mullenberg (Perkin-Elmer Corporation, Eden Prairie, MN, 1979).
11. B. SIEMENSMEYER and J. W. SCHULTZE, *Surf. Interface Anal.* **16** (1990) 309.
12. S. K. SEN, J. RIGA and J. VERBIST, *Chem. Phys. Lett*. **39** (1976) 560.
13. H. O. FINKLEA, in "Semiconductor electrodes", edited by H. O. Finklea (Elsevier, Amsterdam, 1988).

Received 14 October 1996
and accepted 22 May 1997